BIOCHEMISTRY
including biophysical chemistry & molecular biology
Article

Biochemistry **2010,** *49,* 1755–1765 1755
DOI: 10.1021/bi901664h

An RNA Aptamer with High Affinity and High Specificity for the 5S RNA Binding Zinc Finger Proteins TFIIIA and p43[†]

Tristen C. Weiss, Gary G. Zhai, and Paul J. Romaniuk*

Department of Biochemistry and Microbiology, University of Victoria, P.O. Box 3055, Victoria, British Columbia V8W 3P6, Canada

Received September 23, 2009; Revised Manuscript Received January 13, 2010

ABSTRACT: The *Xenopus* zinc finger proteins TFIIIA and p43 bind to 5S RNA in immature oocytes to form 7S and 42S ribonucleoprotein storage particles. To probe the similarities and differences in the RNA binding domains of these two proteins, a library of random RNA molecules was enriched using TFIIIA as the bait protein. One of the abundant aptamers isolated, RNA22, bound to both TFIIIA and p43 derived zinc finger peptides with high affinity and specificity even though the predicted secondary structure of the RNA was unrelated to that of 5S RNA. The interactions of TFIIIA and p43 peptides with RNA22 were compared to their interactions with 5S RNA by characterizing the effects of assay conditions, mutations in RNA22, and mutations in the zinc finger proteins. The similarities and differences in the mechanisms by which these two zinc finger proteins interact with 5S RNA compared to RNA22 suggest they share a common platform for RNA binding with enough flexibility to form specific interactions with both RNAs.

Zinc finger proteins carry out diverse functions in the cell, generally involving specific interactions with DNA, RNA, or protein ligands (*1*, *2*). Some members of this class of proteins are multifunctional, interacting with more than one class of ligand through their zinc finger domains. The first zinc finger protein described, *Xenopus* TFIIIA, binds to the internal control region of the 5S RNA gene as part of the transcriptional initiation complex and is also a component of the 7S ribonucleoprotein (RNP) complex that is used to store 5S RNA in the cytoplasm of immature *Xenopus* oocytes (*3*).

The biological pathway of 5S RNA during oocyte development in *Xenopus* involves the zinc finger protein p43 as well as TFIIIA (*4*−*6*). Like TFIIIA, p43 consists of nine tandem zinc finger motifs and forms a specific, high-affinity complex with 5S RNA (*7*). A role in DNA binding or transcriptional regulation has never been demonstrated for p43. The binary complex of p43 and 5S RNA is a component of the cytoplasmic 42S RNP storage particle, which also consists of tRNAs and the protein p48 (*6*, *8*, *9*). As the oocyte matures, the 5S RNA is released from both the 7S and 42S storage particles and is transported to the nucleolus bound to ribosomal protein L5, this complex then being incorporated into newly assembled 60S ribosomal subunits (*5*, *10*, *11*).

The interactions of TFIIIA and p43 with 5S RNA have been characterized in considerable detail (*7*, *12*−*33*). Although both proteins contain nine tandem zinc finger motifs, there is little sequence similarity between them outside of the conserved amino acids that define the canonical zinc finger motif (*7*). Both proteins bind to 5S RNA with similar, high affinities but utilize different sets of zinc fingers to carry out the binding interaction (*13*, *21*, *25*, *26*, *31*, *33*). Both TFIIIA and p43 rely upon the overall three-dimensional shape of the 5S RNA for binding, but each recognizes different, specific regions of sequence and structure within that framework (*12*, *14*, *16*−*19*, *24*, *25*). These results suggest that the 5S RNA was the driving force for evolution of the two zinc finger proteins involved in the RNA storage process, consistent with the need to maintain conservation of the 5S RNA structure given its functional role in the eukaryotic ribosome.

The common domain structure of TFIIIA and p43, combined with their similar affinities for 5S RNA, suggested to us that the two proteins might share a common RNA binding framework that has been specialized in slightly different ways. If this supposition is correct, it predicts that the two proteins would have the capability to form high-affinity complexes with other common RNA ligands. To investigate this hypothesis, we used *in vitro* selection techniques to derive high-affinity RNA aptamers to TFIIIA and test whether any formed high-affinity complexes with p43.

MATERIALS AND METHODS

Bacterial Strains and Plasmid Vectors. The plasmid vectors pET16b and pET30a were used to express recombinant wild-type and mutant zinc finger proteins in *Escherichia coli* strain BL21 DE3 using methods that have been described elsewhere (*25*, *34*, *35*).

Construction of Zinc Finger Protein Expression Vectors. The construction of plasmid vectors used to express *Xenopus* TFIIIA and the *Xenopus* p43 zinc finger peptides p1−8, p1−4, and p6−9 have been described previously (*33*, *35*). The other zinc finger expressing cDNAs used in this study were constructed by the polymerase chain reaction (PCR) using upstream primers containing a recognition sequence for the restriction enzyme *Nco*I and downstream primers containing a recognition sequence for the restriction enzyme *Eco*RI. PCR products were digested with *Nco*I and *Eco*RI and ligated into plasmid pET30a that had been digested with the same restriction enzymes. Ligation reactions were used to transform *E. coli* strain DH5α, and putative constructs were identified by colony PCR using primers specific

[†]This work was supported by a grant from the Natural Sciences and Engineering Research Council of Canada.
*Corresponding author. Telephone: (250) 721-7088. Fax: (250) 721-8855. E-mail: pjr@uvic.ca.

Published on Web 01/22/2010

to pET30a sequences flanking the multiple cloning site. Plasmids were isolated from appropriate colonies, and the correct plasmid constructs were confirmed by DNA sequencing before protein expression and purification.

A cDNA expressing the four zinc finger domain of human YY1 protein (nucleotides 1354−1725 of Genbank NM003403) was constructed by PCR using a plasmid (ATCC MGC-41844) containing the entire YY1 cDNA as a template. A region encoding the last four zinc fingers of the yeast protein ZAP1 (nucleotides 2483−2836 of the sense direction of Genbank Z49331) was amplified by PCR using yeast genomic DNA as a template. A region encoding the four zinc fingers of the yeast protein AZF1 (nucleotides 535840−536202 of Genbank NC001147) was amplified by PCR using yeast genomic DNA as a template. Truncations of the human ZFY protein containing the cDNA regions encoding zinc fingers 1−8 (designated ZFY1, encoded by nucleotides 1533−2258 of Genbank NM003411) and zinc fingers 6−13 (designated ZFY6, encoded by nucleotides 1998−2699 of Genbank NM003411) were constructed by PCR using a plasmid containing the ZFY cDNA (ATCC-59665) as a template.

Expression and Purification of Recombinant Zinc Finger Proteins. Preparations of N-terminal His-tagged zinc finger proteins were carried out as described previously (*34*). Recombinant *Xenopus* TFIIIA was purified by ion-exchange chromatography on Bio-Rex 70 (*35*). Protein purity was confirmed by polyacrylamide gel electrophoresis, and the concentration of each protein preparation was determined by the method of Bradford (*36*).

Radiolabeling of RNA Ligands. Preparation of radiolabeled 5S RNA and selected RNA aptamers by *in vitro* transcription was carried out as described previously (*37*).

In Vitro Selection of RNA Aptamers for TFIIIA. Selection of RNA aptamers specific for TFIIIA was carried out using a random library of 50mer sequences (*38*). The initial round of selection started with 1.5×10^{13} RNA molecules (250 nM) incubated with 300 nM TFIIIA. The RNA and protein were incubated for 30 min at 4 °C in 100 μL of a buffer containing 50 mM Tris-HCl at pH 8.0, 5 mM $MgCl_2$, 100 mM KCl, 25 μM $ZnCl_2$, 1 mM DTT, 100 μg/mL BSA, and 10 μg/mL poly(dI-dC). The samples were filtered through a nitrocellulose membrane on a dot blot apparatus, and individual dots were cut out and incubated for 3 h at room temperature in 200 μL of a buffer containing 0.5 M ammonium acetate, 1 mM EDTA, and 0.1% SDS to extract the protein-bound RNA. An equal volume of phenol−chloroform (1:1) was added; the sample was mixed by vortexing and then centrifuged briefly to separate the layers. The aqueous layer was transferred to a fresh microcentrifuge tube, and the enriched RNA was precipitated with the addition of 10 μg of carrier glycogen and 3 volumes of cold ethanol. After incubation for 30 min at −70 °C, the RNA was pelleted by centrifugation at 13000 rpm for 15 min. The pellet containing the RNA was dried and dissolved in 20 μL of nuclease-free distilled water.

An enriched RNA library for the next round of selection was generated by RT-PCR and transcription by T7 RNA polymerase (*38*), and the selection was repeated as outlined above. The concentration of RNA and TFIIIA was reduced in each subsequent round of selection until it was determined that no further enrichment of the RNA had occurred after selection round 7 which had an RNA concentration of 1.2 nM and a TFIIIA concentration of 5 nM. Seven rounds of mock selection were carried out in the absence of TFIIIA and resulted in no significant enrichment of the library, indicating that aptamers with affinity for either BSA or nitrocellulose had not been selected.

The PCR product from the final selection round was ligated into the *Sma*I site of pUC18. The ligation reaction was used to transform competent *E. coli* JM109 cells, and individual plasmids were prepared for sequencing from 50 of the resulting colonies on LB agar plates. Potential secondary structures of selected aptamer sequences were determined using mfold (*39*, *40*).

Equilibrium Binding of RNAs to Zinc Finger Proteins. The apparent association constants for the binding of radiolabeled RNAs to zinc finger proteins were determined using a double filter binding assay (*41*). The binding buffer consisted of 20 mM Tris-HCl, pH 7.5 (20 °C), 5 mM $MgCl_2$, 100 mM KCl, 10 μM $ZnCl_2$, 0.5 mM tris(2-carboxyethyl)phosphine hydrochloride, 100 μg/mL BSA, and 1 μg/mL polyA. When the effects of altering binding conditions such as temperature, pH, divalent salt concentration, or monovalent salt concentration were being investigated, the binding buffer was altered accordingly.

The affinity of each zinc finger protein for RNA was determined using three or more independent assays. Apparent dissociation constants (K_d) for the binding of the mutant and wild-type proteins to RNA were calculated by fitting the data to a simple bimolecular equilibrium model using the general curve fitting function of Kaleidagraph software (Synergy Software, Reading, PA) and the equation:

$$\frac{[\text{RNA} - \text{protein}]}{[\text{RNA}]_{\text{total}}} = \frac{[\text{protein}]_{\text{total}}}{[\text{protein}]_{\text{total}} + K_d} \quad (1)$$

where $[\text{RNA}]_{\text{total}} \ll K_d$ and $[\text{RNA}-\text{protein}]/[\text{RNA}]_{\text{total}}$ is reported as the fraction of RNA bound. Association constant (K_a) values were derived as the reciprocal of the measured K_d values and are reported as the mean of three independent determinations with the associated standard deviations. Relative affinities were arrived at by dividing the apparent K_a for the mutant protein by the apparent K_a for the wild-type protein determined in parallel or by dividing the apparent K_a for the mutant RNA by the apparent K_a for the wild-type RNA determined in parallel. The errors for relative affinities are given by the expression $\sigma = \{(\sigma 1/\text{M1})^2 + (\sigma 2/\text{M2})^2\}^{1/2}(\text{M2}/\text{M1})$, where M1 and M2 are the respective association constants for wild-type and mutant protein and the σ values are the corresponding standard deviations for these determinations.

Analysis of the Thermodynamic Parameters of RNA Binding by TFIIIA. The contribution of enthalpy ($\Delta H°$) and entropy ($\Delta S°$) to the free energy of RNA binding by TFIIIA was determined from the temperature dependence of the apparent K_a using van't Hoff plots of $\ln(K_a)$ vs $1/T$. For the interaction of TFIIIA with 5S RNA and RNA22, the plots were significantly nonlinear and were analyzed using eq 2 (*42*), where the change in molar heat capacity is represented by $\Delta C°_{P,\text{obs}}$. T_H and T_S are the temperatures at which enthalpy and entropy make no contribution to the free energy of TFIIIA−RNA complex formation.

$$\ln K_a = (\Delta C°_{P,\text{obs}}/R)((T_H/T) - \ln(T_S/T) - 1) \quad (2)$$

The data in the van't Hoff plots were fit to eq 2 using the general curve fitting function of Kaleidagraph 3.0 software in order to solve for $\Delta C°_{P,\text{obs}}$, T_H, and T_S, and these parameters were then used to calculate the contributions of enthalpy and entropy to the

Group I

1	UUUCUGUGAUCUUUGCUCGGAAUGGCUGUGGGUAU**GGGUGGG**UUGGGCUAG	(6)
2	GCACCCAUGCAGGGCAUAGAUGGGUUU**GGGUGGG**AGAUU**GUGUGGG**CCAA	(3)
3	GCUGAGGAUC**GGGUGGA**CCGUGAAAUUGCGGUAGAG**UGGAGGG**AAAUC	(2)
4	UGGCUGAGACAUGCUAAUGGGUCCAGGGUGUCUGGAA**GGGUGGG**GAGGA	(2)
5	AUCUCUGAUGUGGCAUUCG**AGGUGGG**AAA**GGGUGGG**AUGAGUGCCAACGC	(2)
6	UCGCCAAUUGUGACCCCAGCCCUCAUUUGAGCAGGAAC**UGGUGAA**CGUCC	(1)
7	CGCGGUACUUUCGAGGAAUUGGGA**GGGUGGA**GUGUGGAGCCCGGAGAAC	(1)
8	GGAGGGUU**GGGUGGA**GUAAUAUUCAUACUCUAGAUGGACACGCUAUUGU	(1)
9	UUCCUCGGCAAGCUACAGCAUUUGA**GGCUGGG**GGGGAUU**GGGAGGG**AGUGC	(1)
10	AAUAGUACCGCGAUUGGCCAAAG**GGAUGGG**UC**GGGAGGG**AUUUGGCUGAA	(1)
11	AUGAGCUAUAUUCGCGUGGCGCAUGGAUUGA**GGGAGGG**AUUGCGACUGCG	(1)
12	UAGGUUGCCCCAGCAUG**CGGUGGG**UAUAGA**GGGUGGG**AGGCGAGUGGAC	(1)
13	CUGAUAGAUGCAACGGUGUAAGGGCGAAUGGGUU**GGGUGGG**UAUGAUCA	(1)
14	UGCCAAUCU**UGGUGGG**UGGUAAAUGUGGGAGGGCGUCCUAGAUCUGGC	(1)
15	UUUUCGUGCUCCAAGGCCUGAGGGC**GGGUGGG**UGAAGUUGGUACCUUGGA	(1)
16	AAUGCUAUCCUACGUUU**GGGUGGG**UUU**GGGGGGG**GAUAGACUAAGGA	(1)
17	GUGUUGAGAUGAU**GUGUGGG**UGGGUGUCUUGUA**GGGAGGA**AUCUGACGAC	(1)
18	ACGGUUAUGCCUACUU**GGGCGGG**UUUGG**GUGUGGG**UUGUGAUGGCAGGUC	(1)
19	CUUAGACUCGGGCU**GGGUGGG**UAUGGUGCGGUCGACACGUGGAAAGUAAC	(1)
20	CAUGACAUGCCGCCGGGGUAA**GGGAGGG**CGUUGGGGAUGUCGCAUUGA	(1)

Group II

21	UAAACCUGCUGGCAGUGUGACCUAAGGACCAAGCCGUUCCUGAGGAACGUC	(5)
22	UAAAUCGUUGCUACAUUCCCAAUUGAACGGCCCGGGUUCUUAACACGUGC	(4)
23	CCUACUUGGAUGUGCCAGGACGUCCCUAGACUGAAGUCUGUGACCUAGAG	(2)
24	UACCGUGUGCAAUUGAACGUAAGCUGUCUGUGCUGAAACGUACGGCUUUA	(2)
25	UACGGUAUGCAGUGAGAACGUCUCAACGCCCGCGCCUGUUACGUUGUGAC	(1)
26	CCCUAUGAACGGCCCGGAGUAUAGUUGAUGCUGCUACAGAAAAACUUGGC	(1)
27	UACUAGGCUGCCUAAAGAUACAUGCUAGUUGGUAUACGCUUAGGUGUUAA	(1)
28	UUUAGUGUACGAUCUUUAUCGUAAGAUGCAACUCUCCAGAACUUACUGCU	(1)
29	GCGCGUAAAGAGGUCAGAGCGUUGAUUUGUGCAUUCUUGUGCACCCACCA	(1)
30	CUCAGCCUUUGCGGCUUGAGGGCCCGGAGUAGUUACUACAUUGUAACCCUG	(1)

FIGURE 1: Sequence alignment of 50 RNA aptamers selected by TFIIIA. Group I shows the alignment of 20 unique sequences that share a GGGUGGG consensus motif. Group II shows the 10 unique sequences within the 50 clones that do not contain a GGGUGGG consensus motif. The number in parentheses after each sequence indicates the number of times that sequence occurs within the 50 clones that were sequenced.

free energy of TFIIIA−RNA complex formation as a function of temperature using eqs 3 and 4 (*42*).

$$\Delta H^\circ = \Delta C^\circ_{P,\mathrm{obs}}(T - T_H) \quad (3)$$

$$T\Delta S^\circ = T\Delta C^\circ_{P,\mathrm{obs}}(\ln(T/T_S)) \quad (4)$$

RESULTS

In Vitro Selection of RNA Aptamers for TFIIIA. The *Xenopus* zinc finger protein TFIIIA binds specifically to an internal promoter in the 5S RNA gene and to the 5S RNA transcript (*3*). Specific nucleotides on the 5S RNA and structural elements such as a three-helix junction are necessary for TFIIIA binding (*14*, *16*−*19*, *24*, *30*, *32*). To probe the RNA binding repertoire of TFIIIA further, we conducted an *in vitro* selection experiment using a library of RNA molecules containing a 50 nucleotide long region of random sequence. Seven rounds of selection enriched the library for RNA aptamers that bound to TFIIIA with dissociation constants in the nanomolar range. Fifty individual isolates from the enriched library were sequenced, yielding 30 unique sequences (Figure 1). Two-thirds of the sequences contained a consensus GGGUGGG sequence with RNA1 being present in 6 of the 50 isolates. The other 10 unique sequences contained no obvious consensus motifs; however, RNA21 and RNA22 were present in 5 and 4 copies, respectively. None of the selected aptamer sequences showed any significant similarity to the sequence of 5S RNA.

The RNA aptamer transcripts include fixed sequences that flank the random 50mer region which were used during the selection process to facilitate amplification of selected RNAs after each round (*38*). These sequences are involved along with the selected sequences in folding the RNA aptamers into specific three-dimensional shapes. The three most abundant RNA aptamers for TFIIIA are each predicted to fold into stable structures (*39*, *40*), which are distinctly different from the highly conserved secondary structure of 5S RNA (Figure 2).

Equilibrium Binding of RNA Aptamers to TFIIIA and Other Zinc Finger Proteins. The affinities of RNA1, RNA21, and RNA22 for TFIIIA were determined using an equilibrium binding assay (Figure 3A). RNA1 has the highest affinity for TFIIIA, although RNA21 and RNA22 both bind with affinities that are comparable to 5S RNA, the cognate biological ligand for TFIIIA (Table 1). RNA1 showed poor specificity for TFIIIA and had high affinity for a variety of zinc finger proteins (Figure 3B, Table 1). There is no distinction in affinity for RNA1 between those proteins that bind to 5S RNA with high affinity (TFIIIA, p1−8, p1−4) and those that do not (ZFY1, ZFY6, p6−9, YY1, ZAP1, AZF1). Thus RNA1 is an aptamer with general specificity and high affinity for zinc finger proteins. Further characterization of this novel RNA aptamer and its interactions with zinc finger proteins will be described in a future publication (*43*).

RNA21 exhibited a modest selectivity ratio of 17-fold for TFIIIA and p1−8 compared to the noncognate ZFY6 and 54-fold compared to the noncognate YY1 and AZF1 peptides (Figure 3C, Table 1). The selectivity ratio is greater than 500 for

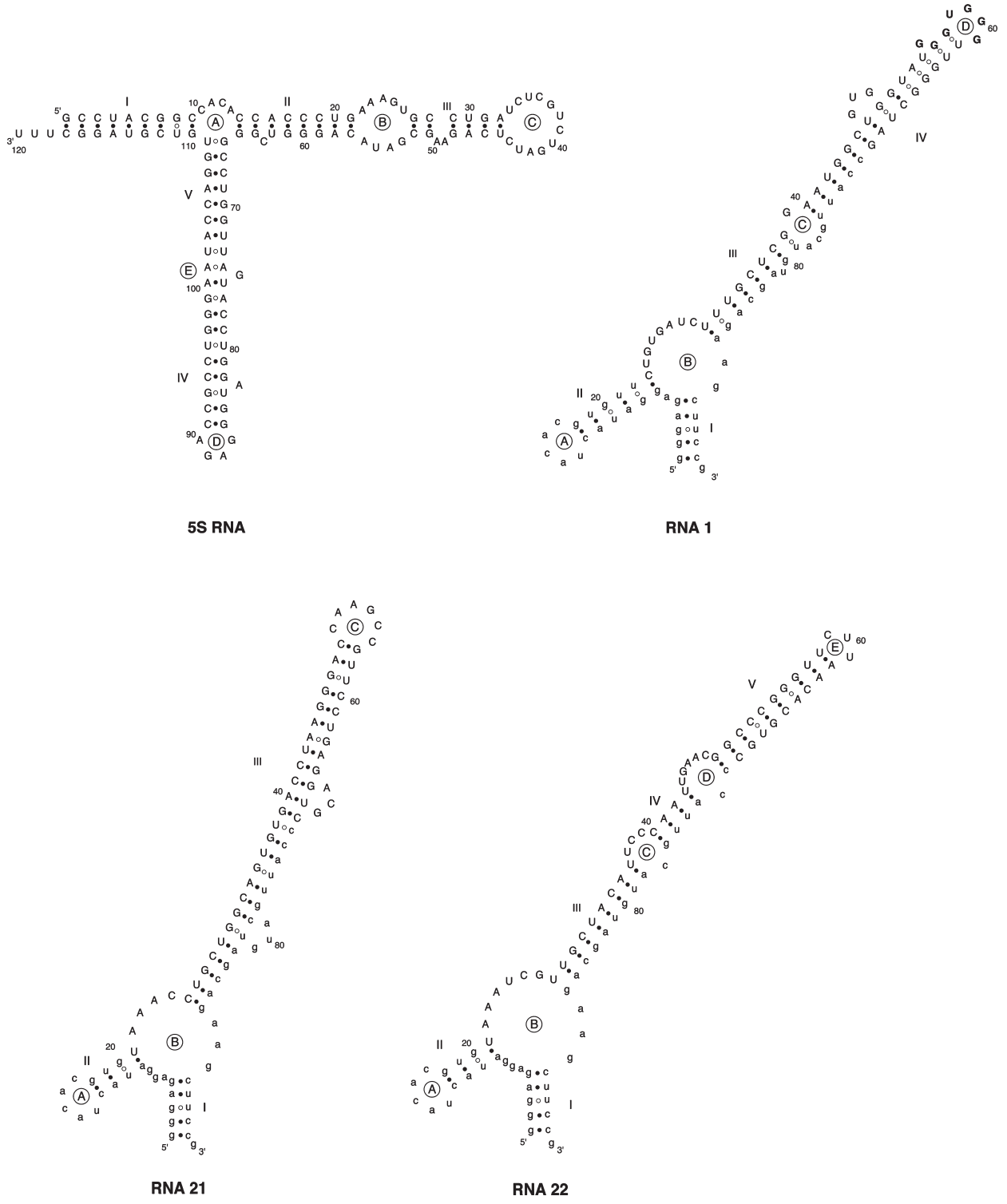

FIGURE 2: A comparison of the secondary structures of 5S RNA and the three most abundant RNA aptamers. Lowest free energy structures were predicted for the aptamers using the mfold program (*39*, *40*). The position of the GGGUGGG consensus motif in RNA1 is indicated by bold letters.

the binding of 5S RNA to the cognate proteins TFIIIA, p1−8, and p1−4 compared to the noncognate proteins ZFY1, ZFY6, p6−9, YY1, ZAP1, and AZF1 (Table 1). Thus RNA21 is less promiscuous than RNA1 in binding zinc finger proteins, showing no demonstrable affinity for either p6−9 or ZFY1 (Table 1).

In comparison to the other two abundant aptamers, RNA22 exhibits selectivity for TFIIIA, p1−8, and p1−4 that is as high as that observed for 5S RNA (Figure 3D, Table 1). These three proteins bind to RNA22 with affinities comparable to their affinities for 5S RNA, whereas the rest of the zinc finger proteins tested have no measurable affinity for RNA22 (Table 1). This result suggests that RNA22 in some way mimics 5S RNA in the binding of TFIIIA, p1−8, and p1−4.

Comparison of Binding Conditions on the Affinities of 5S RNA and RNA22 for TFIIIA and p1−8. Changes in equilibrium binding conditions were used to gain insight into the mechanism of binding of TFIIIA to RNA22 vs 5S RNA

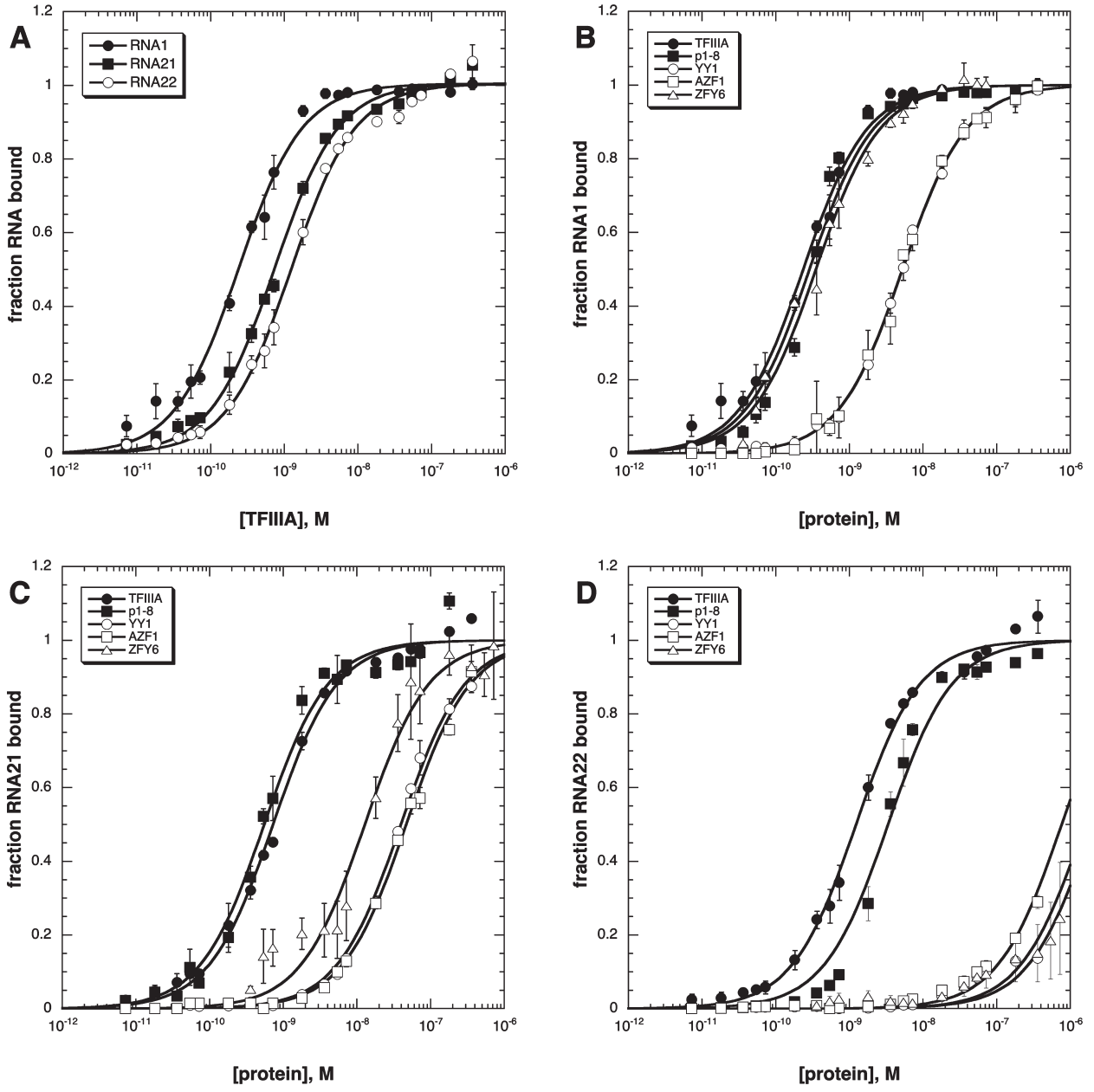

FIGURE 3: (A) Equilibrium binding of aptamers RNA1, RNA21, and RNA22 to TFIIIA. (B) Equilibrium binding of RNA1 to TFIIIA, p1−8, YY1, AZF1, and ZFY6. (C) Equilibrium binding of RNA21 to TFIIIA, p1−8, YY1, AZF1, and ZFY6. (D) Equilibrium binding of RNA22 to TFIIIA, p1−8, YY1, AZF1, and ZFY6. Each data point is the mean value from three independent experiments, with the standard deviation for each point represented by the error bars. Best-fit curves to a simple bimolecular equilibrium are shown.

(Figure 4). Both interactions exhibit a fairly broad optimum for $MgCl_2$ concentration between 1 and 5 mM (Figure 4A). The binding of both RNAs to TFIIIA shows a moderate sensitivity to the concentration of monovalent cations, with 5S RNA being slightly more sensitive than RNA22 (Figure 4B). A precise calculation of the number of ion pairs formed between TFIIIA and each RNA is not possible from these data because it requires too many untested assumptions (*44*−*46*), but the data are consistent with more ion pairs being formed between TFIIIA and 5S RNA than between TFIIIA and RNA22. The binding of TFIIIA to 5S RNA and RNA22 occurs with quite similar, broad pH optima (Figure 4C). This result suggests that there are no differences in the key titratable groups on TFIIIA required for binding to the two RNAs.

The contributions of enthalpy and entropy to the formation of TFIIIA−5S RNA and TFIIIA−RNA22 complexes were determined by measuring the temperature dependence of the apparent association constant (Figure 4D). The nonlinear nature of the data indicated that enthalpy changes with temperature, and the data were fit by nonlinear regression to eq 2 that takes such temperature dependence of enthalpy into account (*42*) (Table 2). At the assay temperature of 20 °C, formation of both TFIIIA−RNA complexes are driven by large enthalpy terms, the enthalpy contribution being greater for the TFIIIA−RNA22 interaction. The free energy of formation of the TFIIIA−RNA22 complex has an unfavorable entropy term at 20 °C, while entropy makes virtually no contribution to the TFIIIA−5S RNA complex formation since the T_S value is essentially equal to the assay temperature (Table 2).

Binding of TFIIIA, p1−*8, and p1*−*4 to Site-Directed Mutants of RNA22*. In forming specific complexes with 5S RNA, TFIIIA and p43 both rely upon the three-dimensional

Table 1: Comparison of the Apparent Dissociation Constants for the Binding of RNA Aptamers and 5S RNA to Zinc Finger Proteins

	K_d (nM)			
protein	RNA1	RNA21	RNA22	5S RNA
TFIIIA	0.24 ± 0.01	0.74 ± 0.06	1.27 ± 0.15	1.00 ± 0.50
p1−8	0.29 ± 0.01	0.61 ± 0.06	3.33 ± 0.40	2.85 ± 0.23
p1−4	1.70 ± 0.17	4.57 ± 0.35	7.13 ± 0.49	2.00 ± 0.18
p6−9	1.77 ± 0.25	> 500[a]	> 500[a]	> 500[a]
YY1	5.33 ± 0.59	39.50 ± 2.12	> 500[a]	> 500[a]
AZF1	5.27 ± 0.75	47.00 ± 0.31	> 500[a]	> 500[a]
ZAP1	1.33 ± 0.06	28.50 ± 3.54	> 500[a]	> 500[a]
ZFY1	0.90 ± 0.46	> 500[a]	> 500[a]	> 500[a]
ZFY6	0.48 ± 0.20	12.72 ± 1.17	> 500[a]	> 500[a]

[a]Apparent K_d for the mutant protein was above 500 nM and could not be measured accurately.

shape of the RNA to provide the context for forming individual bonding contacts unique to each protein−RNA complex (*14*, *16*−*19*, *24*, *30*, *32*). RNA22 is predicted to fold into an extremely stable structure, consisting of two short stems formed by a 5′ fixed flanking sequence and a long stem closing a trinucleotide hairpin loop consisting primarily of the selected sequence (Figure 2). To test the importance of the RNA structure and sequence elements for protein binding, a series of mutations in RNA22 were introduced within the helix IV/V hairpin loop formed by nucleotides 40−76. The first set of mutations (M1−M3) was designed to test the importance of the trinucleotide loop E and the base pairs within helix V that close this loop (Figure 5). Several of the other non GGGUGGG aptamers are also predicted to form a structure with a trinucleotide hairpin loop, suggesting that this structure element might be important for TFIIIA binding. Mutant M1 maintains the hairpin structure

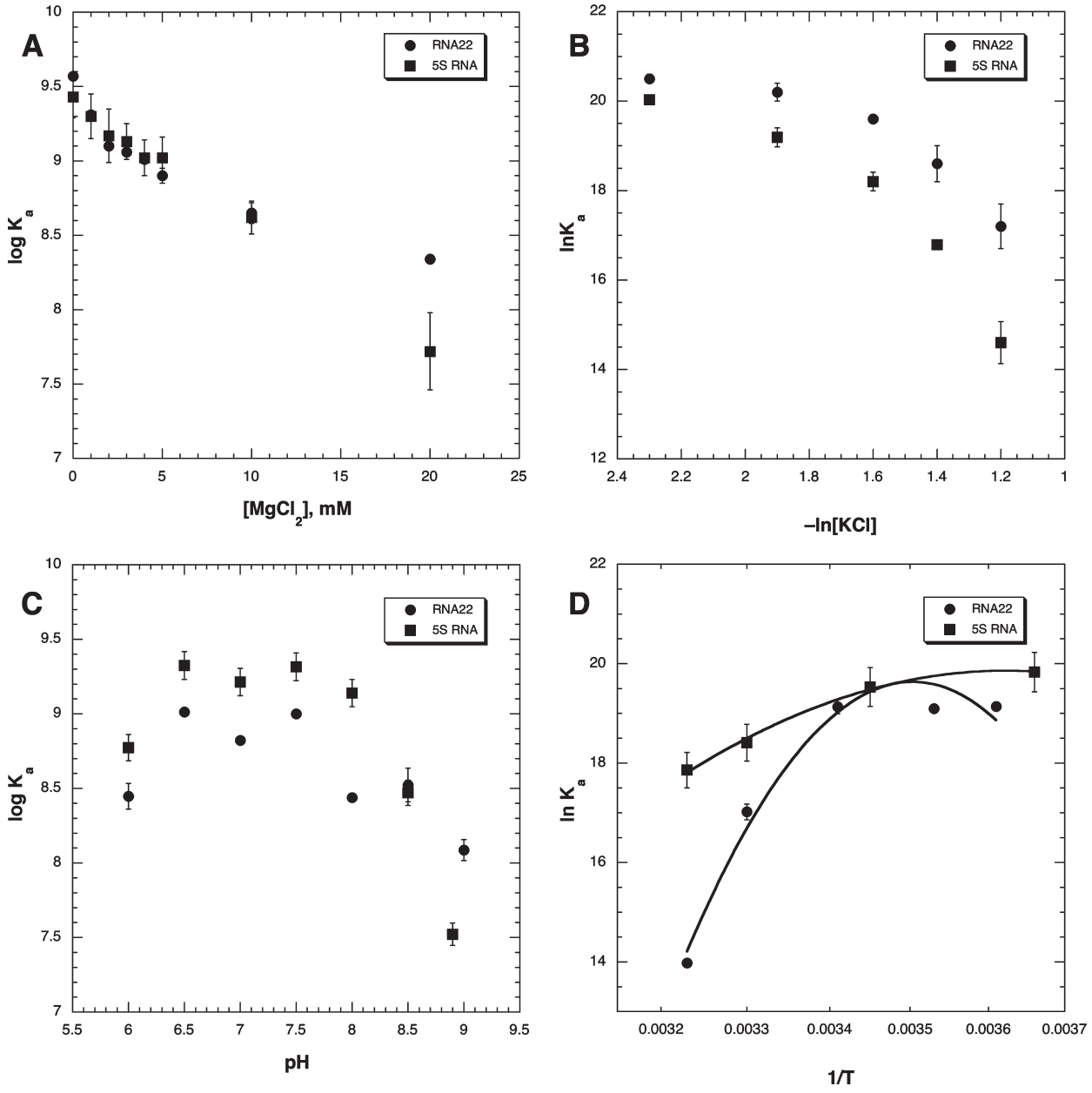

FIGURE 4: Effects of assay conditions on the affinities of TFIIIA for 5S RNA and RNA22. (A) Effect of magnesium ion concentration. (B) Effect of monovalent salt concentration. (C) Effect of pH. (D) Temperature dependence of binding affinity. Each data point is the mean value from three independent experiments, with the standard deviation for each point represented by the error bars. Best-fit curves to a simple bimolecular equilibrium are shown.

Table 2: Thermodynamic Constants for the Interaction of TFIIIA with 5S RNA and RNA22

RNA	$\Delta C°_{P,obs}$[a] (kcal·mol^{-1})	T_H[a] (K)	T_S[a] (K)	$\Delta H°$, 20 °C[b] (kcal·mol^{-1})	$\Delta S°$, 20 °C[c] (cal·deg^{-1}·mol^{-1})
5S RNA	−0.6 ± 0.1	276.1 ± 3.2	293.5 ± 1.2	−10.9 ± 2.5	1.2 ± 2.2
RNA22	−3.4 ± 0.7	285.5 ± 1.8	288.8 ± 1.3	−25.4 ± 6.8	−48.6 ± 15.0

[a]Values were calculated from nonlinear regression analysis of data in Figure 4D using eq 2 and are reported ± standard error of regression. [b]Values were calculated using eq 3 and incorporating errors from $\Delta C°_{P,obs}$ and T_H. [c]Values were calculated using eq 4 and incorporating errors from $\Delta C°_{P,obs}$ and T_S.

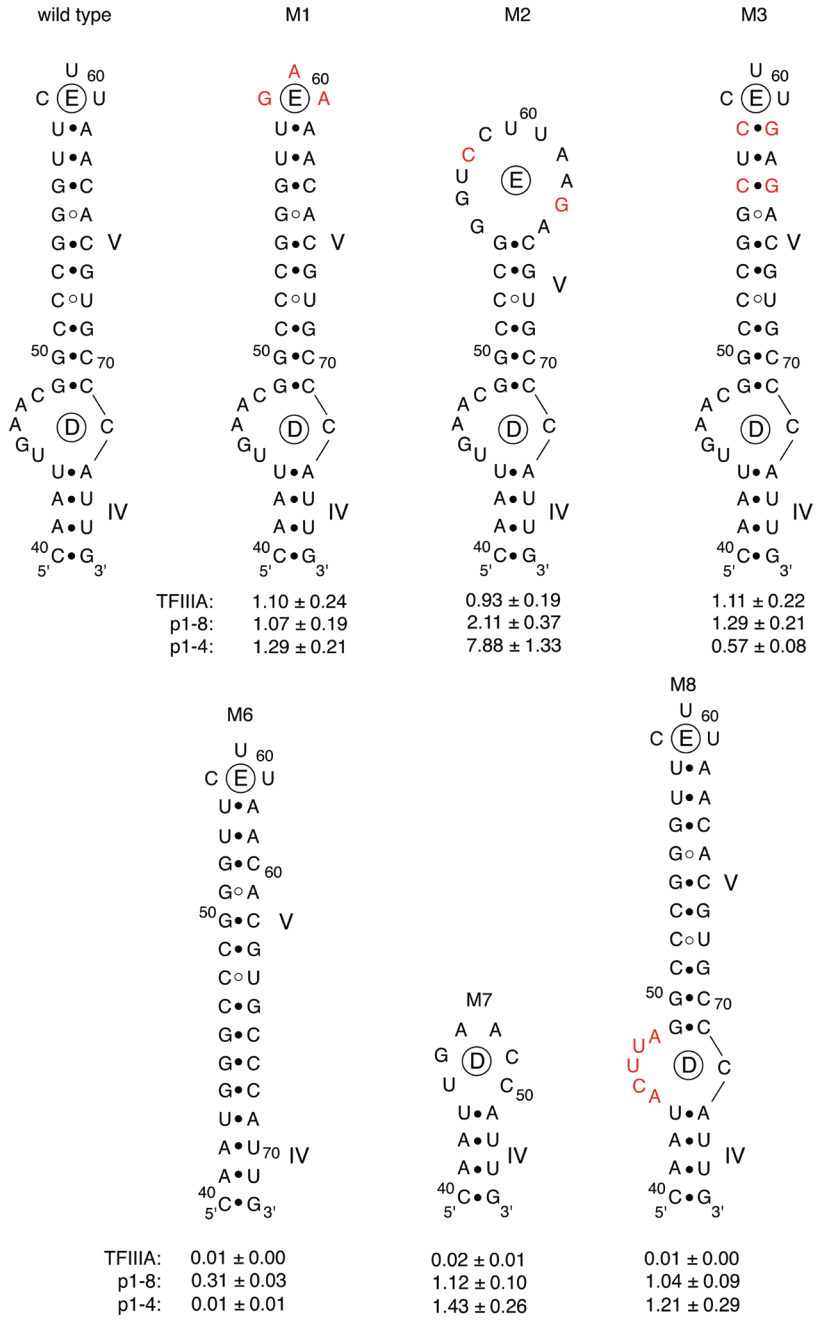

FIGURE 5: Effects of site-directed mutations of the helix IV/loop D/helix V/loop E region of RNA22 on the binding of TFIIIA and the p43-derived zinc finger peptides p1−8 and p1−4. Relative binding affinities were determined from three independent determinations, as outlined in the Materials and Methods section.

but alters the base sequence of loop E. Mutant M2 changes two nucleotides in helix V, resulting in an enlarged hairpin loop, while mutant M3 alters two of the base pairs in helix V that close loop E. None of these mutations significantly altered the affinity of RNA22 for TFIIIA (Figure 5). Mutants M1 and M3 had very little effect on the binding of the p43 zinc finger peptides p1−8 and p1−4, but the enlargement of the hairpin loop in mutant M2 resulted in a 2−8-fold increase in affinity for these two proteins.

One of the key structural elements important for the binding of TFIIIA and p43 to 5S RNA is loop A (Figure 2), which acts as the junction for the three helical stems of the RNA (*14*, *16*−*19*, *24*, *25*, *30*, *32*). In RNA22, nucleotides 44−48 form a single-sided

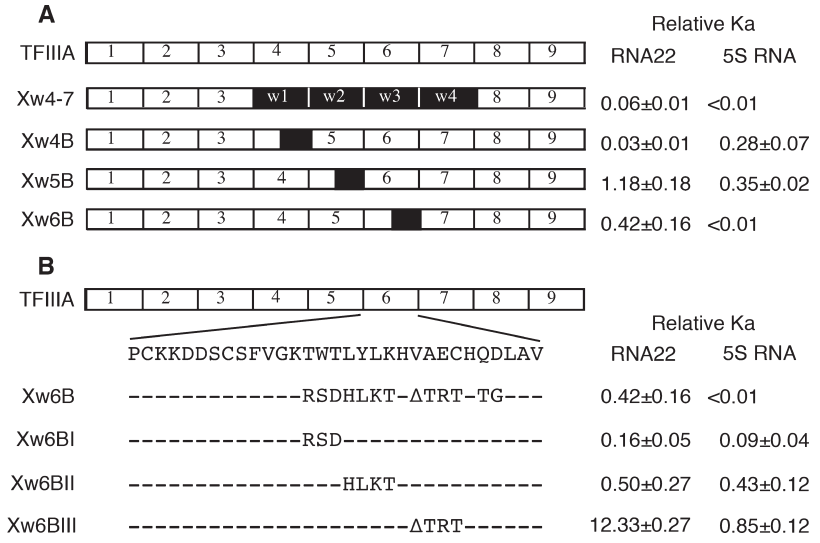

FIGURE 6: A comparison of the effects of site-directed mutations of TFIIIA on RNA22 and 5S RNA binding affinities. (A) The effects of scanning mutations created using zinc finger sequences from the unrelated protein WT1 (black boxes). (B) Amino acid sequence of zinc finger 6 is shown, along with the scanning mutations created within the α-helix of this finger. Relative binding affinities were determined from three independent determinations, as outlined in the Materials and Methods section.

loop D that acts as a junction between helices IV and V (Figure 2). Mutations M4−M6 were created to test the importance of the structure and sequence of this loop for binding of RNA22 to TFIIIA and the p43 zinc finger peptides p1−8 and p1−4 (Figure 5). In mutant M4 nucleotides 44−48 are deleted, resulting in a large decrease in the affinity of TFIIIA and p1−4 for RNA22 and a modest decrease in affinity for p1−8. Deletion of helix V/loop E in mutant M5 also greatly decreases TFIIIA binding, while substitution of nucleotides 44−48 of loop D in mutant M6 also results in a large decrease in the affinity of RNA22 for TFIIIA. In comparison, mutations M5 and M6 have no effect on the affinity of RNA22 for p1−8 and p1−4 (Figure 5).

Comparison of the Effects of Mutations in TFIIIA and p1−4 on Binding to RNA22 and 5S RNA. Previous studies of the interactions of TFIIIA and p43 with 5S RNA identified key amino acids through the analysis of the effects of site-directed mutations in the proteins on RNA binding affinities (*26*, *31*, *33*). The affinities of these same mutant TFIIIA and p43 proteins for RNA22 were measured using the equilibrium binding assay so that the effects of the mutations on RNA22 binding could be compared with the previously obtained data for 5S RNA binding. The series of Xw mutants of TFIIIA are chimeric proteins in which specific regions of TFIIIA are replaced by sequences derived from the unrelated zinc finger protein WT1 (Figure 6) (*31*). As the data in Figure 6 show, fingers 4−6 of TFIIIA are critical to binding both 5S RNA and RNA22. The α-helices of fingers 4 and 6 contribute to the free energies of binding 5S RNA and RNA22, finger 4 being more critical for RNA22 binding. The TWT residues at the start of the α-helix in finger 6 are as important for RNA22 binding as they are for 5S RNA binding (Figure 6). Finger 6 of TFIIIA has two unusual features compared to the canonical zinc finger: four residues instead of three beween the two histidines and a downstream linker that begins with QD rather than TG. In mutant Xw6BIII the histidine spacing of finger 6 is converted to the canonical form by substituting the residues found in finger 3 of WT1 (Figure 6). This mutation had no significant effect on the affinity of TFIIIA for 5S RNA but resulted in a large increase in affinity for RNA22, suggesting that the slight conformational changes to the α-helix configuration in the mutant result in the formation of an additional contact to RNA22.

A similar analysis was previously undertaken to identify key residues in the first four fingers of p43 involved in binding to 5S RNA (*33*), and those mutant proteins were assayed for effects on affinity for RNA22 (Figure 7). Individual finger swap mutations pW1, pW2, pW3, and pW4 previously identified zinc fingers 1 and 4 as being particularly critical for high-affinity binding to 5S RNA. A similar pattern is observed for the binding of these four mutant proteins to RNA22, although the magnitudes of the effects were significantly greater for binding to 5S RNA. The data also indicate that zinc finger 3 contributes more to 5S RNA binding than RNA22 binding (Figure 7). The effects of individual point mutations in zinc finger 1 identified K31 and D34 as key residues for the binding of p1−4 to 5S RNA. The results obtained for RNA22 binding with the same point mutations indicate that E29 is particularly critical for the interaction with p1−4 (Figure 7). Point mutations in zinc finger 4 identified K119, K120, and R121 as 5S RNA contacting residues while assaying the same mutant proteins for RNA22 affinity identified K119 and R121 as important, although the effects of the mutations were an order of magnitude smaller for RNA22 than 5S RNA (Figure 7).

DISCUSSION

The fact that both TFIIIA and p43 consist of nine tandem zinc fingers and each binds with high affinity and specificity to 5S RNA in the absence of any sequence homology suggested the possibility that the two proteins might share a common RNA binding platform. To test this hypothesis, we carried out multiple rounds of *in vitro* selection of high-affinity RNA aptamers from a random library, using TFIIIA as the bait protein. Of the three most abundant aptamers that accounted for 30% of the library, only RNA22 replicated the high affinity and specificity of 5S RNA not only for TFIIIA, the bait protein, but also for the 5S RNA binding peptides p1−8 and p1−4 derived from p43.

A comparison of the equilibrium binding of TFIIIA to 5S RNA and RNA22 indicated that these interactions are generally quite similar in response to changes in monovalent and divalent

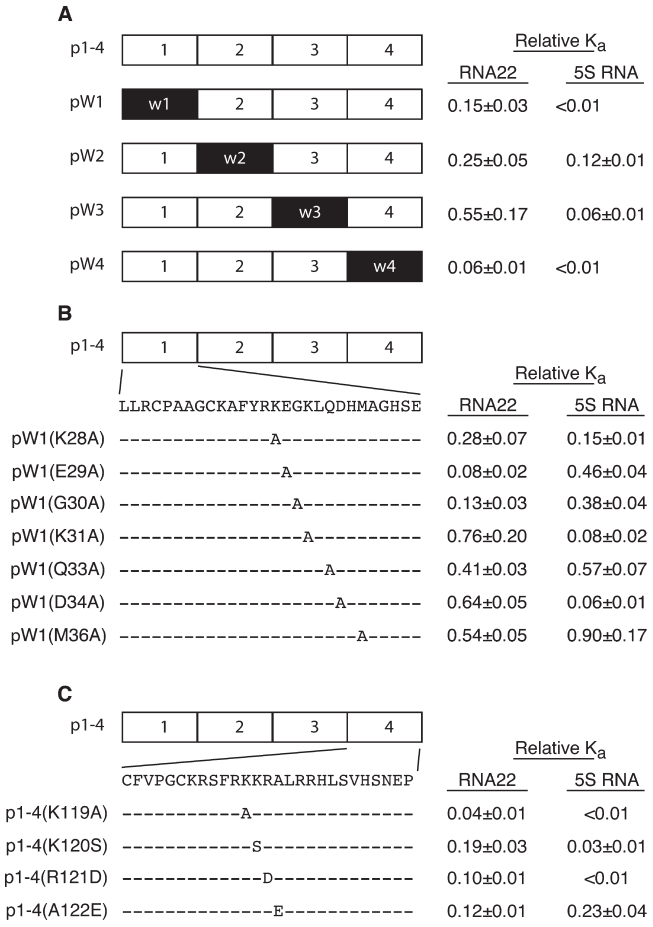

FIGURE 7: A comparison of the effects of site-directed mutations of the p43-derived zinc finger peptide p1−4 on RNA22 and 5S RNA binding affinities. (A) The effects of scanning mutations created using zinc finger sequences from the unrelated protein WT1 (black boxes). (B) Amino acid sequence of zinc finger 1 of p43 is shown, along with the point mutations created within the α-helix of this finger. (C) Amino acid sequence of zinc finger 4 of p43 is shown, along with the point mutations created within the α-helix of this finger. Relative binding affinities were determined from three independent determinations, as outlined in the Materials and Methods section.

ions, with the TFIIIA−5S RNA interaction being somewhat more sensitive to higher concentrations of both types of ions. Both interactions show quite similar, broad pH optima, suggesting that there are no significant differences in the roles of titratable groups on TFIIIA in the interactions of the protein with both RNAs. The interaction of TFIIIA with both RNAs is driven by a favorable enthalpy, the contribution of enthalpy to the free energy of binding being greater for RNA22 than it is for 5S RNA. This greater enthalpy overcomes an unfavorable entropy in the TFIIIA−RNA22 interaction and results in similar free energies of binding for the two TFIIIA−RNA interactions. All of these observations are consistent with the conclusion that RNA22 acts as a suitable mimic of 5S RNA in the interaction with TFIIIA.

The structure of 5S RNA consists of three helical stems that meet at a common loop junction, two of the stems closing hairpin loops (Figure 2). TFIIIA interacts with the central portion of the helix IV−V stem structure and the loop A helical junction (*14*, *15*, *17*, *18*, *24*, *30*, *32*). Thus both structure and specific sequence elements in 5S RNA are critical for TFIIIA binding. RNA22 does not share any significant sequence homology with *Xenopus* 5S RNA, nor does the secondary structure predicted for RNA22 show any strong similarities to the well-characterized structure for 5S RNA. Yet the interaction of RNA22 with TFIIIA has the same hallmarks as the 5S RNA interaction with TFIIIA. Neither the hairpin loop E at the end of the long arm of RNA22 nor the double base pairs within helix V that close the hairpin are critical for binding of TFIIIA. However, the structure and base sequence of loop D in the long arm are important for high-affinity binding of TFIIIA to RNA22. This asymmetrical internal loop may adopt a highly accessible conformation like loop A in 5S RNA, allowing TFIIIA to form contacts with the bases within the loop.

In the interaction of TFIIIA with 5S RNA, key contacts with the RNA are formed by residues in zinc fingers 4 and 6 (*26*, *31*, *32*). Within finger 6, a TWT motif at the start of the α-helix forms hydrogen-bonding and stacking interactions with the bases of loop A (*32*). The two threonine residues form hydrogen bonds to the cytosine base at nucleotide 10, while the tryptophan stacks on the adenine base at position 11, which is exposed in the structure of the three helix junction(*32*). This motif is just as critical for the interaction of TFIIIA with RNA22. It is interesting that a mutation further down the α-helix of zinc finger 6 results in an increased affinity of TFIIIA for RNA22, but not 5S RNA. If the interaction of zinc finger 6 with RNA22 occurs at loop D, something about the length, base sequence, and conformation of this loop must allow for a fortuitous interaction with one of the amino acid substitutions in the TFIIIA mutant Xw6BIII. While zinc finger 5 does not appear to be specifically involved in the interaction of TFIIIA with either RNA22 or 5S RNA, residues in the α-helix of zinc finger 4 contribute more to the free energy of binding to RNA22 compared to 5S RNA. In the interaction of TFIIIA with 5S RNA, four amino acids at the tip of zinc finger 4 form hydrogen-bonding contacts to the base and sugar of G75, an extrahelical nucleotide found in the loop E region of the RNA (*32*). In the structure predicted for RNA22, there is no obvious single extrahelical residue in the vicinity of loop D, which suggests that the interaction of zinc finger 4 with RNA22 does not mimic the interaction formed with 5S RNA. The larger free energy contribution of zinc finger 4 to the interaction of TFIIIA with RNA22 compared to 5S RNA suggests that a more extensive interaction occurs between RNA22 and the α-helix of this finger.

Both TFIIIA and p43 have nine zinc fingers and bind to 5S RNA with identical affinities, which is consistent with the equal distribution of stored 5S RNA in the 7S and 42S RNPs (*25*). However, the majority of the free energy of binding of TFIIIA to 5S RNA is contributed by zinc fingers 4 and 6, while in p43 the majority of the free energy of binding to 5S RNA is contributed by zinc fingers 1, 3, and 4 (*31*, *33*). The features of the 5S RNA that are important for the binding of each protein differ (*17*, *24*, *32*). These observations, taken in conjunction with the similar domain structure of p43 and TFIIIA, suggest that the two proteins have a structurally similar RNA binding platform. Within this common structure, each protein relies on unique residues to contact different features of the 5S RNA. The data obtained with the RNA22 aptamer is consistent with such a model. TFIIIA and the p43 peptide p1−8, which contains the key RNA binding zinc fingers, bind to RNA22 with similar affinities, as they do to 5S RNA. Most of the RNA22 binding affinity observed for p1−8 is retained when the peptide is truncated to just the first four zinc fingers of p43, as was observed previously for 5S RNA binding (*33*). Yet p1−8 and p1−4

respond differently to the RNA22 mutants compared to TFIIIA. Most of the mutations tested had little or no effect on p1−8 and p1−4 binding, even in cases where TFIIIA binding was significantly decreased. Deletion of loop D in RNA22 did reduce affinity for both p1−8 and p1−4, but altering the sequence of this loop did not affect the binding of these two proteins. Just like 5S RNA, different features of RNA22 are critical for the formation of interactions with the TFIIIA and the p43 zinc fingers.

Some amino acids of TFIIIA were found to be critical for binding to both 5S RNA and RNA22, while others were critical for just the 5S RNA interaction or the RNA22 interaction. A similar trend was observed for the p43 peptide p1−4. Finger swapping mutations identified fingers 1, 3, and 4 as being critical for 5S RNA binding, with the largest contribution to binding coming from fingers 1 and 4 (*33*). For RNA22 binding, finger 3 does not seem to be critical, and while fingers 1 and 4 are important the magnitude of the effect of the finger swap mutation in each case was less for RNA22 binding than it was for 5S RNA binding. Within the α-helix of finger 1, residues K28, K31, and D34 are particularly important for 5S RNA binding (*33*), while for RNA22 binding the key residues are K28, E29, and G30. These three residues occur at the start of the α-helix of zinc finger 1, suggesting that this finger is tipped toward RNA22 in a fashion analogous to the orientation of TFIIIA zinc fingers 4 and 6 toward 5S RNA (*32*). Within the α-helix of zinc finger 4, residues K119, K120, and R121 are critical for binding of p1−4 to 5S RNA (*33*). The interaction of zinc finger 4 of p1−4 with RNA22 is particularly dependent upon K119, while K120, R121, and A122 all play equivalent, but slightly less important roles in binding.

Isolation of RNA aptamers that bind with high affinity and specificity to nucleic acid binding proteins, but which lack sequence and structural similarity to the target protein's biological ligand, has been reported previously (*47*−*53*). Detailed structural comparisons of aptamer−protein and biological ligand−protein complexes have been carried out for bacteriophage MS2 coat protein and eukaryotic transcription factor NF-κB. These comparisons revealed that the complexes share a common binding interface that in the case of the aptamer complexes leads to the formation of many but not all of the specific bonding contacts observed in the biological ligand complexes (*47*, *48*, *50*, *52*). The biochemical comparison presented here comparing the interaction of RNA22 and 5S RNA with TFIIIA indicates that the aptamer and 5S RNA also share a common binding interface in which many but not all of the bonding interactions formed are common to both complexes. What is remarkable about RNA22 is its ability to interact with high affinity and specificity to the RNA binding zinc fingers of p43. While TFIIIA and p43 both bind to 5S RNA in the immature *Xenopus* oocyte, they utilize different zinc fingers and different specific features of the 5S RNA to form their respective complexes, a characteristic replicated in their interactions with RNA22. Since RNA22 was isolated from an *in vitro* selection experiment that utilized only TFIIIA as the bait protein, its ability to bind to p43 zinc fingers suggests that despite the differences in the two proteins and their interactions with 5S RNA they must share a common RNA binding interface with sufficient flexibility to allow for highly specific interactions with more than one RNA. This observation has interesting implications for the evolution of the 5S RNA storage system in the immature oocytes of amphibia.

ACKNOWLEDGMENT

The authors thank Jill Turner and Ioana Rosu for technical assistance.

REFERENCES

1. Ladomery, M., and Dellaire, G. (2002) Multifunctional zinc finger proteins in development and disease. *Ann. Hum. Genet. 66*, 331–342.
2. Laity, J. H., Lee, B. M., and Wright, P. E. (2001) Zinc finger proteins: new insights into structural and functional diversity. *Curr. Opin. Struct. Biol. 11*, 39–46.
3. Pelham, H. R. B., and Brown, D. D. (1980) A specific transcription factor that can bind either the 5S RNA gene or 5S RNA. *Proc. Natl. Acad. Sci. U.S.A. 77*, 4170–4174.
4. Denis, H., and Mairy, M. (1972) Recherches biochimiques sur l'oogenese: 1. Distribution intracellulaire du RNA dans les petits oocytes de *Xenopus laevis*. *Eur. J. Biochem. 25*, 524–534.
5. Mairy, M., and Denis, H. (1972) Recherches biochimiques sur l'oogenèse: 2. Assemblage des ribosomes pendant le grand accroissement des oocytes de *Xenopus laevis*. *Eur. J. Biochem. 25*, 535–543.
6. Picard, B., le Maire, M., Wegnez, M., and Denis, H. (1980) Biochemical research on oogenesis: composition of the 42S storage particles of *Xenopus laevis* oocytes. *Eur. J. Biochem. 109*, 359–368.
7. Joho, K. E., Darby, M. K., Crawford, E. T., and Brown, D. D. (1990) A finger protein structurally similar to TFIIIA that binds exclusively to 5S RNA in *Xenopus*. *Cell 61*, 293–300.
8. Kloetzel, P.-M., Whitfield, W., and Sommerville, J. (1981) Analysis and reconstitution of an RNP particle which stores 5S RNA and tRNA in amphibian oocytes. *Nucleic Acids Res. 9*, 605–621.
9. Barrett, P., Kloetzel, P.-M., and Sommerville, J. (1983) Specific interaction of proteins with 5S RNA and tRNA in the 42S storage particle of *Xenopus* oocytes. *Biochim. Biophys. Acta 740*, 347–354.
10. Murdoch, K. J., and Allison, L. A. (1996) A role for ribosomal protein L5 in the nuclear import of 5S rRNA in *Xenopus* oocytes. *Exp. Cell. Res. 227*, 332–343.
11. Rudt, F., and Pieler, T. (1996) Cytoplasmic retention and nuclear import of 5S ribosomal RNA containing RNPs. *EMBO J. 15*, 1383–1391.
12. Pieler, T., Erdmann, V. A., and Appel, B. (1984) Structural requirements for the interaction of 5S rRNA with the eukaryotic transcription factor IIIA. *Nucleic Acids Res. 12*, 8393–8406.
13. Romaniuk, P. J. (1985) Characterization of the RNA binding properties of transcription factor IIIA of *Xenopus laevis* oocytes. *Nucleic Acids Res. 13*, 5369–5387.
14. Pieler, T., Guddat, U., Oei, S. L., and Erdmann, V. A. (1986) Analysis of the RNA structural elements involved in the binding of the transcription factor IIIA from *Xenopus laevis*. *Nucleic Acids Res. 14*, 6313–6327.
15. Romaniuk, P. J., de Stevenson, I. L., and Wong, H.-H. A. (1987) Defining the binding site of *Xenopus* transcription factor IIIA on 5S RNA using truncated and chimeric 5S RNA molecules. *Nucleic Acids Res. 15*, 2737–2755.
16. Baudin, F., and Romaniuk, P. J. (1989) A difference in the importance of bulged nucleotides and their parent base pairs in the binding of transcription factor IIIA to *Xenopus* 5S RNA and 5S RNA genes. *Nucleic Acids Res. 17*, 2043–2056.
17. Romaniuk, P. J. (1989) The role of highly conserved single-stranded nucleotides of *Xenopus* 5S RNA in the binding of transcription factor IIIA. *Biochemistry 28*, 1388–1395.
18. Baudin, F., Romaniuk, P. J., Romby, P., Brunel, C., Westhof, E., Ehresmann, B., and Ehresmann, C. (1991) Involvement of hinge nucleotides of *Xenopus laevis* 5S rRNA in the RNA structural organization and in the binding of transcription factor TFIIIA. *J. Mol. Biol. 218*, 69–81.
19. You, Q., Veldhoen, N., Baudin, F., and Romaniuk, P. J. (1991) Mutations in 5S DNA and 5S RNA have different effects on the binding of *Xenopus* transcription factor IIIA. *Biochemistry 30*, 2495–2500.
20. Clemens, K. R., Liao, X. B., Wolf, V., Wright, P. E., and Gottesfeld, J. M. (1992) Definition of the binding sites of individual zinc fingers in the transcription factor IIIA-5S RNA gene complex. *Proc. Natl. Acad. Sci. U.S.A 89*, 10822–10826.
21. Darby, M. K., and Joho, K. E. (1992) Differential binding of zinc fingers from *Xenopus* TFIIIA and p43 to 5S RNA and the 5S RNA gene. *Mol. Cell. Biol. 12*, 3155–3164.
22. Theunissen, O., Rudt, F., Guddat, U., Mentzel, H., and Pieler, T. (1992) RNA and DNA binding zinc fingers in *Xenopus* TFIIIA. *Cell 71*, 679–690.

23. Clemens, K. R., Wolf, V., Mcbryant, S. J., Zhang, P. H., Liao, X. B., Wright, P. E., and Gottesfeld, J. M. (1993) Molecular basis for specific recognition of both RNA and DNA by a zinc finger protein. *Science 260*, 530–533.
24. McBryant, S. J., Veldhoen, N., Gedulin, B., Leresche, A., Foster, M. P., Wright, P. E., Romaniuk, P. J., and Gottesfeld, J. M. (1995) Interaction of the RNA binding fingers of *Xenopus* transcription factor IIIA with specific regions of 5 S ribosomal RNA. *J. Mol. Biol. 248*, 44–57.
25. Zang, W. Q., and Romaniuk, P. J. (1995) Characterization of the 5S RNA binding activity of *Xenopus* zinc finger protein p43. *J. Mol. Biol. 245*, 549–558.
26. Zang, W. Q., Veldhoen, N., and Romaniuk, P. J. (1995) Effects of zinc finger mutations on the nucleic acid binding activities of *Xenopus* transcription factor IIIA. *Biochemistry 34*, 15545–15552.
27. Setzer, D. R., Menezes, S. R., Del Rio, S., Hung, V. S., and Subramanyan, G. (1996) Functional interactions between the zinc fingers of *Xenopus* transcription factor IIIA during 5S rRNA binding. *RNA 2*, 1254–1269.
28. Ryan, R. F., and Darby, M. K. (1998) The role of zinc finger linkers in p43 and TFIIIA binding to 5S rRNA and DNA. *Nucleic Acids Res. 26*, 703–709.
29. Theunissen, O., Rudt, F., and Pieler, T. (1998) Structural determinants in 5S RNA and TFIIIA for 7S RNP formation. *Eur. J. Biochem. 258*, 758–767.
30. Searles, M., Lu, D., and Klug, A. (2000) The role of the central zinc fingers of transcription factor IIIA in binding to 5S RNA. *J. Mol. Biol. 301*, 47–60.
31. Hamilton, T. B., Turner, J., Barilla, K., and Romaniuk, P. J. (2001) Contribution of individual amino acids to the nucleic acid binding activities of the *Xenopus* zinc finger proteins TFIIIA and p43. *Biochemistry 40*, 6093–6101.
32. Lu, D., Searles, M. A., and Klug, A. (2003) Crystal structure of a zinc finger-RNA complex reveals two modes of molecular recognition. *Nature 426*, 96–100.
33. Bhatia, S. S., Weiss, T. C., and Romaniuk, P. J. (2008) Contribution of individual amino acids to the 5S RNA binding activity of the *Xenopus* zinc finger protein p43. *Biochemistry 47*, 8398–8405.
34. Hamilton, T., Barilla, K., and Romaniuk, P. (1995) High affinity binding sites for the Wilms' tumour suppressor protein WT1. *Nucleic Acids Res. 23*, 277–284.
35. Veldhoen, N., You, Q. M., Setzer, D. R., and Romaniuk, P. J. (1994) Contribution of individual base pairs to the interaction of TFIIIA with the *Xenopus* 5S RNA gene. *Biochemistry 33*, 7568–7575.
36. Bradford, M. M. (1976) A rapid and sensitive method for the quantitation of microgram quantities of protein utilizing the principle of protein-dye binding. *Anal. Biochem. 72*, 248–254.
37. Zhai, G., Iskandar, M., Barilla, K., and Romaniuk, P. J. (2001) Characterization of RNA aptamer binding by the Wilms' tumor suppressor protein WT1. *Biochemistry 40*, 2032–2040.
38. Ciesiolka, J., Illangasekare, M., Majerfeld, I., Nickles, T., Welch, M., Yarus, M., and Zinnen, S. (1996) Affinity selection-amplification from randomized ribooligonucleotide pools. *Methods Enzymol. 267*, 315–335.
39. Mathews, D. H., Sabina, J., Zuker, M., and Turner, D. H. (1999) Expanded sequence dependence of thermodynamic parameters improves prediction of RNA secondary structure. *J. Mol. Biol. 288*, 911–940.
40. Zuker, M. (1989) On finding all suboptimal foldings of an RNA molecule. *Science 244*, 48–52.
41. Hall, K. B., and Kranz, J. K. (1999) Nitrocellulose filter binding for determination of dissociation constants. *Methods Mol. Biol. 118*, 105–114.
42. Ha, J. H., Spolar, R. S., and Record, M. T., Jr. (1989) Role of the hydrophobic effect in stability of site-specific protein-DNA complexes. *J. Mol. Biol. 209*, 801–816.
43. Weiss, T. C., Zhai, G. G., Bhatia, S. S., and Romaniuk, P. J. (2010) An RNA with high affinity and broad specificity for zinc finger proteins, Biochemistry (to be published).
44. Lohman, T. M., deHaseth, P. L., and Record, M. T., Jr. (1980) Pentalysine-deoxyribonucleic acid interactions: a model for the general effects of ion concentrations on the interactions of proteins with nucleic acids. *Biochemistry 19*, 3522–3530.
45. Record, M. T., Jr., Anderson, C. F., and Lohman, T. M. (1978) Thermodynamic analysis of ion effects on the binding and conformational equilibria of proteins and nucleic acids: the roles of ion association or release, screening, and ion effects on water activity. *Q. Rev. Biophys. 11*, 103–178.
46. Record, M. T., Jr., Lohman, T. M., and de Haseth, P. (1976) Ion effects on ligand-nucleic acid interactions. *J. Mol. Biol. 107*, 145–158.
47. Convery, M. A., Rowsell, S., Stonehouse, N. J., Ellington, A. D., Hirao, I., Murray, J. B., Peabody, D. S., Phillips, S. E., and Stockley, P. G. (1998) Crystal structure of an RNA aptamer-protein complex at 2.8 Å resolution. *Nat. Struct. Biol. 5*, 133–139.
48. Ghosh, G., Huang, D. B., and Huxford, T. (2004) Molecular mimicry of the NF-kB DNA target site by a selected RNA aptamer. *Curr. Opin. Struct. Biol. 14*, 21–27.
49. Hesselberth, J. R., Miller, D., Robertus, J., and Ellington, A. D. (2000) *In vitro* selection of RNA molecules that inhibit the activity of ricin A chain. *J. Biol. Chem. 275*, 4937–4942.
50. Huang, D. B., Vu, D., Cassiday, L. A., Zimmerman, J. M., Maher, L. J., III, and Ghosh, G. (2003) Crystal structure of NF-kB (p50)2 complexed to a high affinity RNA aptamer. *Proc. Natl. Acad. Sci. U.S.A. 100*, 9268–9273.
51. Lebruska, L. L., and Maher, L. J., III (1999) Selection and characterization of an RNA decoy for transcription factor NF-kB. *Biochemistry 38*, 3168–3174.
52. Parrott, A. M., Lago, H., Adams, C. J., Ashcroft, A. E., Stonehouse, N. J., and Stockley, P. G. (2000) RNA aptamers for the MS2 bacteriophage coat protein and the wild type RNA operator have similar solution behaviour. *Nucleic Acids Res. 28*, 489–497.
53. Spingola, M., Lim, F., and Peabody, D. S. (2002) Recognition of diverse RNAs by a single protein structural framework. *Arch. Biochem. Biophys. 405*, 122–129.